THE JOURNAL OF BIOLOGICAL CHEMISTRY
Vol. 271, No. 43, Issue of October 25, pp. 26602–26608, 1996
Printed in U.S.A.

Kinetic Interconversion of Rat and Bovine Homologs of the α Subunit of an Amiloride-sensitive Na^+ Channel by C-terminal Truncation of the Bovine Subunit*

(Received for publication, May 21, 1996, and in revised form, July 17, 1996)

Catherine M. Fuller‡, Iskander I. Ismailov, Bakhram K. Berdiev, Vadim G. Shlyonsky, and Dale J. Benos

From the Department of Physiology and Biophysics, University of Alabama at Birmingham, Birmingham, Alabama 35294

We have recently cloned the α subunit of a bovine amiloride-sensitive Na^+ channel (αbENaC). This subunit shares extensive homology with both rat and human αENaC subunits but shows marked divergence at the C terminus beginning at amino acid 584 of the 697-residue sequence. When incorporated into planar lipid bilayers, αbENaC almost exclusively exhibits a main transition to 39 picosiemens (pS) with very rare 13 pS step transitions to one of two subconductance states (26 and 13 pS). In contrast, the α subunit of the rat renal homolog of ENaC (αrENaC) has a main transition step to 13 pS that is almost constituitively open, with a second stepwise transition of 26 to 39 pS. A deletion mutant of αbENaC, encompassing the entire C-terminal region (R567*X*), converts the kinetic behavior of αbENaC to that of αrENaC, *i.e.* a transition to 13 pS followed by a second 26 pS transition to 39 pS. Chemical cross-linking of R567*X* restores the wild-type αbENaC gating pattern, whereas treatment with the reducing agent dithiothreitol produced only 13 pS transitions. In contrast, an equivalent C-terminal truncation of αrENaC (R613*X*) had no effect on the gating pattern of αrENaC. These results are consistent with the hypothesis that interactions between the C termini of αbENaC account for the different kinetic behavior of this member of the ENaC family of Na^+ channels.

A family of amiloride-sensitive Na^+ channels, the ENaCs, has recently been cloned from the colon of rats either fed a low sodium diet or treated with dexamethasone, and they have since been identified in both epithelial and non-epithelial tissues from several species (1–8). This family of channels is comprised of three homologous subunits, termed α, β, and γ, that when co-expressed in *Xenopus* oocytes produce maximum amiloride-sensitive channel activity (2). However, the α subunit alone can act as an amiloride-sensitive Na^+ channel (9), and other related members of the ENaC family can form a conductive pore by expression of a single cDNA (10–12). We have recently cloned the α subunit of the bovine renal homolog of ENaC, which we term αbENaC[1] (13). This bovine isoform also forms an amiloride-sensitive Na^+ channel when expressed in *Xenopus* oocytes. Fusion of αbENaC-expressing oocyte membrane vesicles to the planar lipid bilayer reveals an amiloride-sensitive Na^+ channel that exhibits a distinct kinetic signature. This is characterized by a main transition to 39 pS, with very rare 13 pS step transitions to one of two subconductance states (26 and 13 pS). Moreover, there are long (1–5 min) closed periods between bursts of activity. In contrast, the rat colon αENaC subunit (the first cloned member of the ENaC family), exhibits a very different kinetic profile when studied under identical conditions. In this case, the main transition step is to 13 pS with a second stepwise transition of 26 to 39 pS (9), and there are no long closures. Although both αbENaC and αrENaC share an identical domain organization, are of similar size, and are highly homologous at the nucleotide level over most of their length, there are some specific differences (2, 13). The most notable among these is a marked sequence (and thus amino acid) divergence at their respective C termini. This divergence initiates at residue 584 in αbENaC (residue 630 in αrENaC) and continues to the end of the coding region. The open reading frame of αbENaC also initiates 44 amino acids downstream of the αrENaC start site and terminates 23 amino acids downstream of the αrENaC stop. We therefore tested the hypothesis that the C-terminal divergence between αbENaC and the prototypical αrENaC accounts for the difference in the gating pattern exhibited by these two Na^+ channel proteins. We have thus constructed C-terminal truncated versions of both αENaC subunits, expressed the respective cRNAs in *Xenopus* oocytes, and fused oocyte membrane vesicles to the planar lipid bilayer for electrophysiological recording.

EXPERIMENTAL PROCEDURES

Materials

Molecular reagents were obtained from Promega (Madison, WI), New England Biolabs Inc. (Beverly, MA), Stratagene (La Jolla, CA), or Bio 101, Inc. (Buena Vista, CA). Female *Xenopus laevis* were obtained from Xenopus I (Ann Arbor, MI). Radioactive [^{35}S]methionine was from DuPont NEN. Lipids for planar bilayer experiments were purchased from Avanti Polar Lipids (Birmingham, AL). All other reagents were obtained either from Sigma, Bio-Rad, or Fisher.

Methods

Truncation of ENaC cDNA—We adopted a PCR-based strategy to generate truncation mutants of αrENaC and αbENaC. The full-length (2.1 kilobases) αbENaC open reading frame was used as a template in a PCR reaction, using primers designed to insert a stop codon at amino acid residue 567 in the αbENaC sequence. This residue falls just after the predicted end of the second transmembrane domain of the α subunit. The primer pairs (including *Bgl*II sites) were 5′-GAAGATCTTC**ATG**AAGGGAGACAAGCCTGA-3′ (sense) and 5′-GAAGATCTTCT-

* This study was supported by National Institutes of Health Grant DK37206. The costs of publication of this article were defrayed in part by the payment of page charges. This article must therefore be hereby marked "*advertisement*" in accordance with 18 U.S.C. Section 1734 solely to indicate this fact.

‡ To whom correspondence should be addressed: Dept. of Physiology and Biophysics, University of Alabama at Birmingham, BHSB 735, University Station, Birmingham, AL 35294-0005. Tel.: 205-934-6085; Fax: 205-934-2377; E-mail: fuller@phybio.bhs.uab.edu.

[1] The abbreviations used are: αbENaC, α subunit of the bovine renal homolog of ENaC; pS, picosiemen(s); αrENaC, α subunit of the rat renal homolog of ENaC; PCR, polymerase chain reaction; DTT, dithiothreitol; MOPS, 4-morpholinepropanesulfonic acid; DTNB, 5,5′-dithiobis-(2-nitrobenzoate).

```
                                          1  MLDHTR  6 rat

APELNIDLDLHASNSPKGSMKGNQFKEQDPCPPQPMQGLGKGDKREEQGL 56 rat
                                              ||||.||.|
                                        1 MKGDKPEEPGP 11 bovine

GPEPSAPRQPTEEEEALIEFHRSYRELFQFFCNNTTIHGAIRLVCSKHNR 106 rat
|||||:|..|||||||:||||||||||:|||||||||||||||||.|||
GPEPSGPPPPTEEEEALLEFHRSYRELFEFFCNNTTIHGAIRLVCSQHNR  61 bovine

MKTAFWAVLWLCTFGMMYWQFALLFEEYLSYPVSLNINLNSDKLVFPAVT 156 rat
|||.||||||||||||||||: ||:||:|||||||||||||||||||||.
MKTVFWAVLWLCTFGMMYWQFGQLFGEYFSYPVSLNINLNSDKLVFPAVS 111 bovine

VCTLNPYRYTEIKEELEELDRITEQTLFDLYKYNSSYPRQAGARRRSSRD 206 rat
:|||||||||.||.|||||||||||||||||||||||||  :  .|: ||.||
ICTLNPYRYKEIQEELEELDRITEQTLFDLYKYNSS..KTLVAHARSRRD 159 bovine

LLGAFPHPLQRLRTPPPPYSGRTGAAGLPAYATTIPQVDRKDWKIGFQLC 256 rat
| :::|||||||..|:||..:|..  : ..  .. |||:||||||||||
LREPLPHPLQRLPVPAPPHAARGVRRAGSSMRDNNPQVNRKDWKIGFQLC 209 bovine

NQNKSDCFYQTYSSGVDAVREWYRFHYINILSRLS.DTSPALEEEALGNF 305 rat
|||||||||||||||||||||||||||||||||| . ||||.|||:.||.|
NQNKSDCFYQTYSSGVDAVREWYRFHYINILSRRRQDTSPSLEEDVLGKF 259 bovine

IFTCRFNQAPCNQANYSKFHHPMYGNCYTFNDKNNSNLWMSSMPGVNNGL 355 rat
||||||||..||:||||.|||||||||||||.|||||||||||||||
IFTCRFNQDSCNEANYSHFHHPMYGNCYTFNDKNSSNLWMSSMPGVNNGL 309 bovine

SLTLRTEQNDFIPLLSTVTGARVMVHGQDEPAFMDDGGFNLRPGVETSIS 405 rat
|||||||||||||||||||||||||||:.|||||||:|||||||||||||
SLTLRTEQNDFIPLLSTVTGARVMVHERDEPAFMDDAGFNLRPGVETSIS 359 bovine

MRKEALDSLGGNYGDCTENGSDVPVKNLYPSKYTQQVCIHSCFQENMIKK 455 rat
|.|||:|.|||:|||||.|||:|||.|||  .|||||||||||||.|||.
MSKEAVDRLGGDYGDCTKNGSEVPVENLYNTKYTQQVCIHSCFQESMIKE 409 bovine

CGCAYIFYPKPKGVEFCDYRKQSSWGYCYYKLQGAFSLDSLGCFSKCRKP 505 rat
||||||||||:|.||||||||||:.|||||||||||:||| |.|||||.|||||
CGCAYIFYPRPDGVEFCDYRKHNSWGYCYYKLQDAFSSDRLGCFTKCRKP 459 bovine

CSVINYKLSAGYSRWPSVKSQDWIFEMLSLQNNYTINNKRNGVAKLNIFF 555 rat
|||. |||||:||.|||..||||:|:||| |||||.|||:|||||||||
CSVTIYKLSASYSQWPSATSQDWVFQMLSRQNNYTIKNKRDGVAKLNIFF 509 bovine

KELNYKTNSESPSVTMVSLLSNLGSQWSLWFGSSVLSVVEMADVIFDLLV 605 rat
||||||.||||||||||.|||||||||||||||||||||||||||::|:||||
KELNYKSNSESPSVTMVTLLSNLGSQWSLWFGSSVLSVVEMAELIIDLLV 559 bovine

ITLLMLLRRFRSRYWSPGRGARGAREVASTPASSFPSRFCPHPTSPPPSL 655 rat
||:|||||||||||||||::|.|       |   ||:.| .  ||||:
ITFLMLLRRFRSRYWSPGRGGKGTR...RWLHS...SRLPPLQFLPPPSF 603 bovine

.........PQQGMTPP...LALTAPPPAYATLGPSAP............ 681 rat
         . .|:..|   |. .:||:.   ||.:..
LLLIPARPCHLPGLVSPSTCLCHPGPPPSSIRLGRGQHLCPRSGGALREG 653 bovine

..PLDSAAP..DCSACALAALstop                           698 rat
  ||..|:.  :....|||::
RYPLPKAGTSLGGRDAALAGFKNVWRLPVRAAQLPLVCAWVAGRstop   697 bovine
```

FIG. 1. **Alignment of amino acid sequences for rat and bovine αENaC subunits.** The start of αbENaC is shifted 44 amino acids downstream of the αrENaC start site. The two sequences exhibit a high degree of homology until residue position 584 of αbENaC, at which point the sequences begin to diverge. The site of the residue change (R→STOP) is highlighted in *bold* in each sequence.

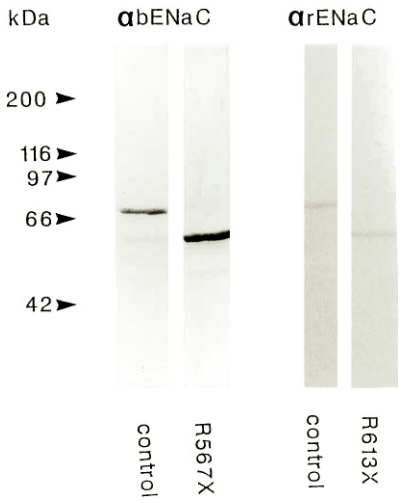

FIG. 2. ***In vitro* translation of wild-type and truncated rat and bovine αENaC subunits.** αENaC cDNAs were transcribed and *in vitro* translated in the presence of [^{35}S]methionine as described under "Methods." *In vitro* translated αbENaC and αrENaC migrated with an M_r of 70,000–75,000 on 8% SDS-polyacrylamide gel electrophoresis. Truncated αbENaC and αrENaC migrated at 54 and 57 kDa, respectively. The autoradiogram was exposed to the gel for 45 min at −80 °C.

T**ATC**CGGAGCAGCAT-3′ (antisense) and extended from bases 1–20 and 1689–1701 of the αbENaC sequence, respectively. PCR was carried out as described previously (13), using Vent DNA polymerase (New England Biolabs Inc.) under the following conditions: 94 °C for 3 min (1 cycle), 94 °C for 1 min, 52 °C for 1 min, 72 °C for 3 min (30 cycles), and 72 °C for 15 min (1 cycle). A PCR product of the predicted size (1726 base pairs) was gel purified, cut with *Bgl*II, phosphorylated, and ligated into pGEM II as described previously (13). In the case of the αrENaC truncation, we used the ExSite mutagenesis kit from Stratagene to create a C-terminal deletion initiating at nucleotide base 1190 of αrENaC. The primer pair consisted of 5′-**TGA**GAGAGGAGAAGGATCC-3′ and 5′-GTAGCAG**CAT**GAGAAGTGTGA-3′ for sense and antisense primers, respectively. The PCR conditions were: 94 °C for 4 min, 58 °C for 2 min, 72 °C for 2 min (1 cycle), 94 °C for 1 min, 58 °C for 2 min, 72 °C for 1 min (8 cycles), and 72 °C for 5 min (1 cycle). The PCR reaction also included 4% formamide to decrease secondary structure. In each case, the mutations resulted in the insertion of a premature stop codon one residue after the predicted termination of the second transmembrane domain of the αENaC subunit. In the case of αbENaC, this is at amino acid 567 (R567*X*), and for αrENaC, the termination falls at amino acid 613 (R613*X*). The respective cRNAs were transcribed from *Bam*HI-linearized plasmid cDNA using a Ribomax T7 polymerase kit from Promega or SP6 polymerase in the presence of a methylguanosine cap analog, $m^7G(5')ppp(5')G$. *In vitro* translation was carried out in the presence of L-[^{35}S]methionine using micrococcal nuclease-treated rabbit reticulocyte lysate (Promega) in the absence of canine pancreatic microsomes (13). *In vitro* translated products were separated by 8% SDS-polyacrylamide gel electrophoresis according to the method of Laemmli (14) under reducing (50 mM DTT) conditions.

Oocyte Injection and Planar Lipid Bilayer Recording—Xenopus oocytes were prepared and injected as described previously (13, 15). Briefly, oocytes were defolliculated in oocyte Ringer (in mM: 82.5 NaCl, 2.4 KCl, 5 $MgCl_2$, 5 HEPES, pH 7.4) containing 1 mg/ml Type 1A collagenase (320 units/mg; Sigma) for 2 h with one solution change. Stage V/VI oocytes were selected and maintained for 24 h in 0.5 × L-15 medium containing 15 mM HEPES and 2% of a 10,000 units/ml solution of penicillin/streptomycin. Oocytes were injected with either 50 nl of nuclease-free water or 50 nl of water + 25 ng of the appropriate cRNA. After an additional 24–48 h, membrane vesicles were prepared from the injected oocytes and frozen at −80 °C for subsequent fusion to the lipid bilayer for physiological recording as described previously (15–17). Planar bilayer membranes were composed of a mixture of diphytanoyl phosphatidylethanolamine/diphytanoyl phosphatidylserine/oxidized cholesterol (20 mg/ml) in a 2:1:2 (w/w/w) ratio, bathed with symmetrical solutions of 100 mM NaCl and 10 mM MOPS (pH 7.5). Data analysis was as described previously (9).

RESULTS

The full-length open reading frames (including the stop codons) of αbENaC and αrENaC are 2,094 and 2,097 base pairs, respectively, predicting translated polypeptides of 697 and 698 amino acids. As shown in Fig. 1, both αbENaC and αrENaC are highly homologous over most of their length. However, this homology breaks down at residue 584 of αbENaC. Under reducing conditions, *in vitro* translated αbENaC and αrENaC migrated with an M_r of 70,000–75,000 (in the absence of co-translational glycosylation), consistent with a predicted size of 79 kDa. As shown in Fig. 2, truncation of the last 130 amino acids in the case of αbENaC and 85 amino acids in the case of αrENaC resulted in both a translated αbENaC product that migrated at 54 kDa and αrENaC product that migrated at 57 kDa.

When membrane vesicles prepared from oocytes expressing R567*X* αbENaC were fused to planar lipid bilayers, we observed a marked difference in the gating pattern of the resultant channel as compared with that found when full-length

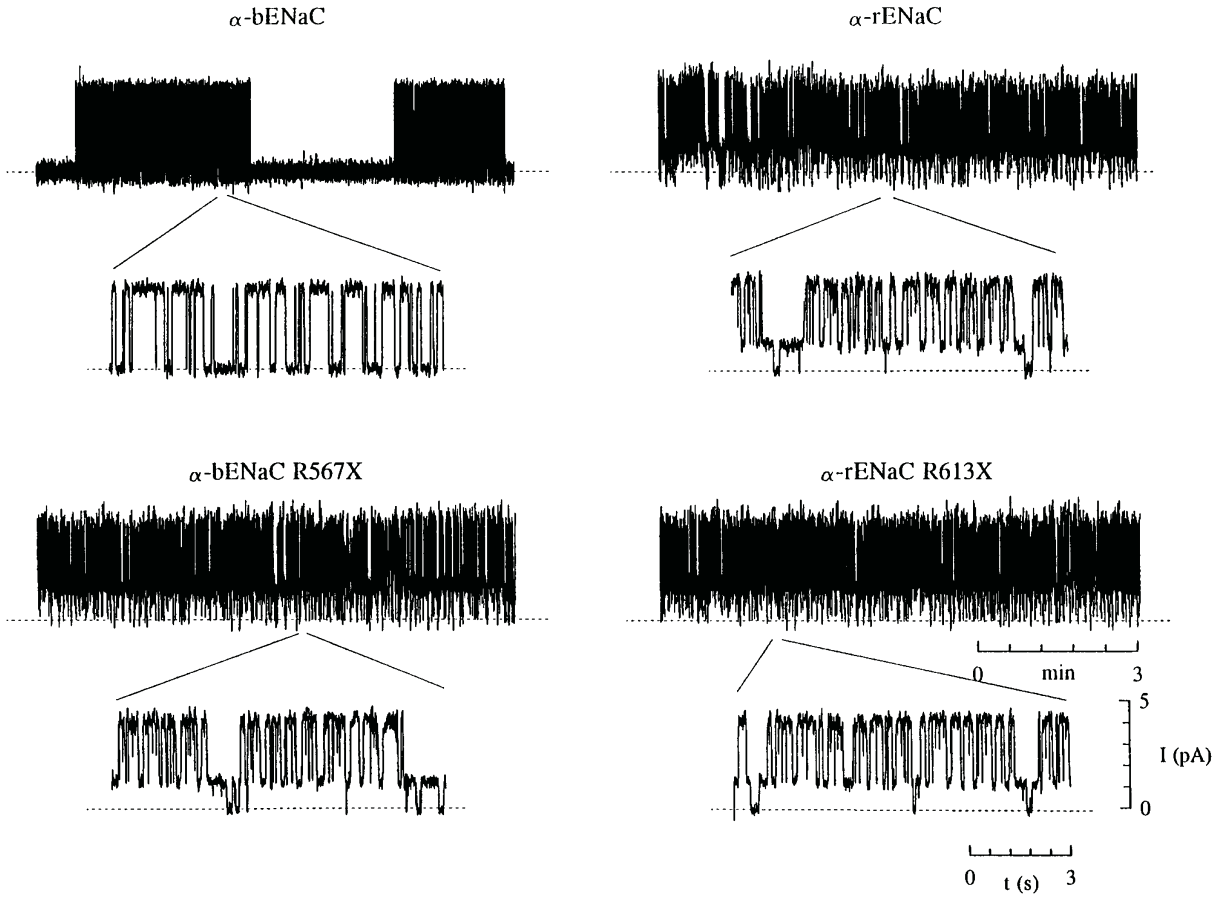

FIG. 3. **Single channel records of both wild-type and C-terminal truncated αbENaC and αrENaC.** The cRNAs for each construct were injected and expressed in *Xenopus* oocytes as described. Oocyte vesicles were then fused to planar lipid bilayers, resulting in the incorporation of ENaC channels into the bilayer membrane. Wild-type αbENaC exhibited predominantly single-step transitions of 39 pS. In contrast, R567*X* αbENaC had an almost constitutively open 13 pS conductance level on top of which were frequent 26 pS transitions to a 39 pS conductance main state. These two states gated cooperatively in that we never observed transitions to 26 pS followed by a second transition of 13 pS. Wild-type αrENaC also exhibited an almost constitutively open 13 pS conductance level, with frequent 26 pS transitions to 39 pS. This gating behavior of αrENaC was identical to that shown by the C-terminal truncated αrENaC construct, R613*X* αrENaC. *Each panel* is representative of at least six separate experiments, the holding potential was +100 mV, and *dashed lines* represent the zero current level.

αbENaC was studied under identical conditions. Control or wild-type αbENaC exhibited a predominantly 39 pS open state conductance (Fig. 3), manifested as a single transition to 39 pS. This channel also exhibited burst-type behavior in that the frequent opening of the 39 pS conductance state was punctuated by long closed periods with little or no channel activity. In contrast, R567*X* αbENaC seemed to show an almost constitutively open 13 pS conductance state, on top of which were frequent 26 pS transitions to 39 pS. In addition, the long periods of closure characteristic of wild-type αbENaC were missing from the gating pattern of the mutant. The kinetic pattern of truncated R567*X* αbENaC was thus virtually identical to that exhibited by wild-type αrENaC, which also showed both a predominantly 13 pS open state conductance with frequent single step transitions of 26 to 39 pS and a lack of burst activity. This kinetic behavior of αrENaC was not further altered by the R613*X* mutation that results in an equivalent C-terminal truncation to R567*X* αbENaC. In both cases, the stepwise transitions of 13 and 26 pS do not follow a binomial distribution (data not shown). Because we never observed the appearance of the 26 pS state independently of the 13 pS transition, these data suggest that, for both wild-type and truncated αrENaC and αbENaC, channel gating exhibits cooperativity.

We have previously shown that exposure of a single wild-type αrENaC incorporated into the planar lipid bilayer to the reducing agent DTT caused the gating behavior of the channel to change radically from 13 and 39 pS main states to 3 × 13 pS subconductance states that appear to gate independently, thus following a binomial distribution (9). Treatment of the wild-type αrENaC with high salt (1.5 M NaCl) also changed the kinetic pattern of gating, increasing the frequency with which the 13 and 26 pS subconductance states were seen. Thus, instead of predominantly observing a single 39 pS transition, the gating pattern could be clearly resolved into 13 and 26 pS components that gated independently (9). Because R567*X* αbENaC seemed to share the gating characteristics of the wild-type αrENaC channel, we examined whether this resemblance could be extended to the behavior of both wild-type and R567*X* αbENaC in the presence of DTT or high salt. As shown in Fig. 4, 50 μM DTT added to the *trans* side of the bilayer (the putative external face of the channel) resolved the wild-type channel into three independently gated 13 pS subconductance states. In the presence of 1.5 M NaCl, wild-type αbENaC showed behavior identical to that exhibited by wild-type αrENaC studied under the same conditions, *i.e.* separately gated 13 and 26 pS transitions. Conversely, the addition of 300 μM 5,5′-dithiobis(2-nitrobenzoate) (DTNB), a sulfhydryl cross-linking agent, to wild-type αbENaC did not affect the gating pattern of the channel. Similarly, the addition of DTT or 1.5 M NaCl to R567*X* αbENaC (Fig. 5) had effects similar to those observed when wild-type αbENaC was used, *i.e.* an increase in

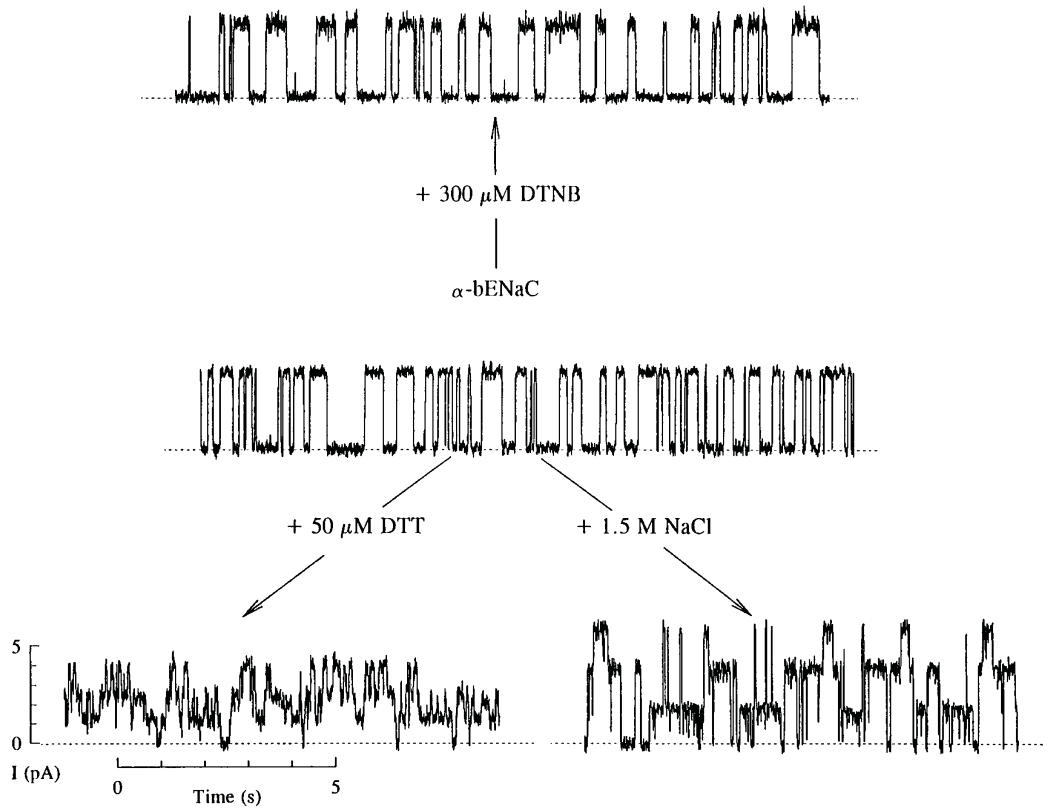

FIG. 4. **Effect of sulfhydryl-active agents and high salt on kinetic behavior of wild-type αbENaC.** Exposure of αbENaC to the disulfide-reducing agent DTT changed channel gating from a single main state conductance of 39 pS to three independently gated 13 pS subconductance states. The addition of high salt (1.5 M NaCl) also changed the gating pattern of wild-type αbENaC such that the 39 pS main state gated independently as one 13 pS and one 26 pS subconductance state, *i.e.* it was possible to observe the 26 pS transition in the absence of an initial transition to 13 pS. The disulfide cross-linking agent DTNB had no effect on the wild-type gating pattern of wild-type αbENaC. *Panels* are representative of eight independent experiments, the holding potential was +100 mV, and *dashed lines* represent the zero current level.

independently gated single step transitions to 13 pS (in the presence of DTT) or an increased appearance of independent 13 and 26 pS transitions (in the presence of 1.5 M NaCl). However, cross-linking with DTNB restored the previously observed gating behavior of wild-type αbENaC, such that only single transitions to 39 pS were observed. Thus, following cross-linking with DTNB, the gating behavior of R567*X* αbENaC was indistinguishable from wild-type αbENaC gating kinetics. An identical gating pattern was also observed when wild-type αrENaC was studied under the same conditions, *i.e.* single step transitions to 39 pS in the presence of 300 μM DTNB (9).

Similarly, when the equivalent truncation mutant of αrENaC (R613*X* αrENaC) was examined under identical conditions to those described above for R567*X* αbENaC, we found that the gating pattern of the mutant was indistinguishable from the pattern exhibited by the wild-type αrENaC channel protein. Thus, as shown in Fig. 6, the addition of 50 μM DTT to R613*X* αrENaC (which in the absence of DTT exhibited an almost constitutively open 13 pS state, with frequent 26 pS transitions to 39 pS) resolved the gating pattern into three independently gated 13 pS subconductance states, while high salt (1.5 M NaCl) altered the gating pattern so that two clear independent states could be observed, one at 13 pS and one at 26 pS. Addition of the cross-linker DTNB resulted in the predominant appearance of a single 39 pS transition (Fig. 6).

We also examined whether other properties characteristic of αbENaC and αrENaC, such as amiloride sensitivity and ion selectivity, were altered in the C-terminal truncated proteins. As shown in Fig. 7, the apparent K_i of amiloride for wild-type αrENaC (168.9 ± 46.1 nM) was not affected in R613*X* αrENaC (K_i = 176.5 ± 48.9 nM). Similarly, the apparent K_i of amiloride for wild-type αbENaC was not affected by C-terminal truncation of the channel (apparent amiloride K_i for wild-type αbENaC was 109.7 ± 32.4 nM as opposed to 113 ± 32.2 nM for R567*X* αbENaC) although the dose-response curve was displaced slightly (but not significantly) to the left of that for αrENaC. In addition, deletion of the C-terminal region of each isoform did not appear to affect the Na^+ to K^+ permeability; P_{Na}:P_K was 10:1 when determined under biionic conditions for both wild-type and truncated αENaC rat and bovine isoforms (Fig. 8).

DISCUSSION

We have previously reported that αrENaC, the α subunit of an amiloride-sensitive Na^+ channel cloned from the rat colon, exhibits a distinct kinetic signature when incorporated into planar lipid bilayers (9). This kinetic signature was identical to that observed when *Xenopus* oocytes heterologously expressing αrENaC were examined under cell-attached patch-clamp conditions (9). The kinetic signature of the channel incorporated into planar lipid bilayers was radically changed by the addition of a disulfide-reactive agent or by the chaotropic effects of high salt. Our earlier studies demonstrated that a single αrENaC channel that predominantly exhibited 13 and 39 pS main state conductances could be resolved into three apparently independently gated 13 pS subconductance states, following reduction of the protein with DTT. Conversely the 39 pS main state conductance could be restored by the addition of a disulfide cross-linker. The effect of high salt was to cause the 13 and 26 pS transition steps to gate independently. Similar effects of disulfide-active agents and high salt were seen when single αβγrENaC channels were studied under identical conditions.

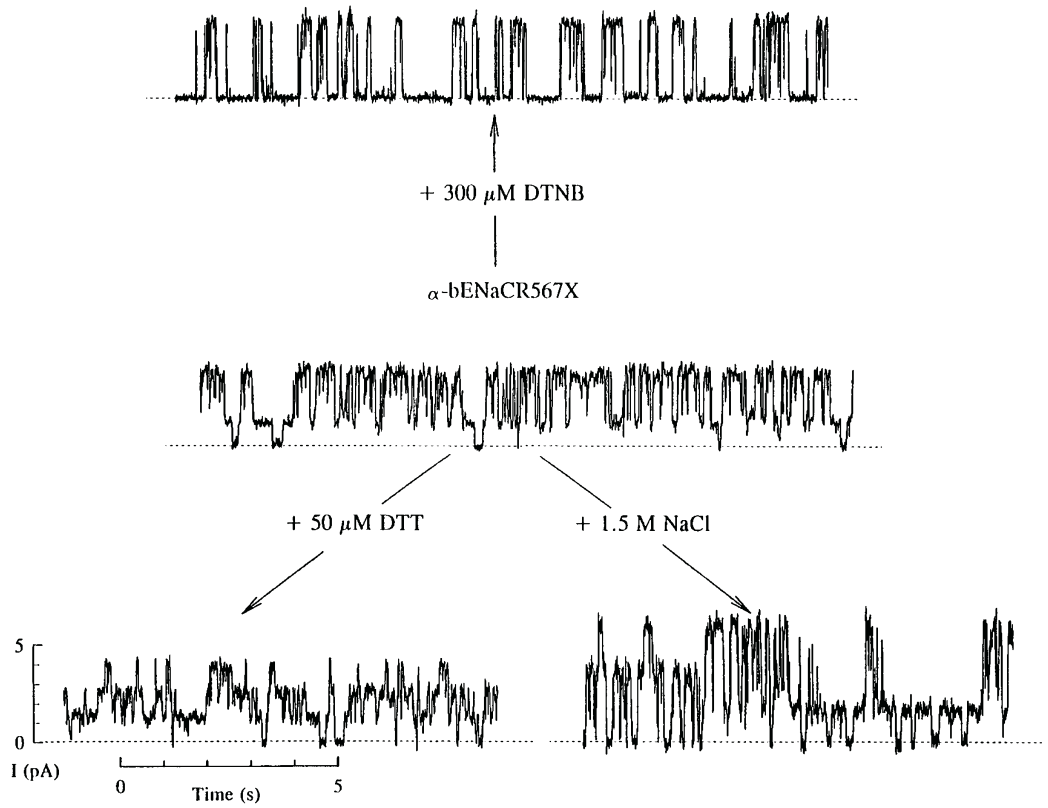

FIG. 5. **Effect of sulhydryl-active agents and high salt on the kinetic behavior of R567*X* αbENaC.** Exposure of truncated αbENaC to the reducing agent DTT changed channel gating from two main conductance levels, that appeared to gate cooperatively, to three independently gated 13 pS conductance states. The addition of 1.5 M NaCl also changed the gating pattern of R567*X* αbENaC such that the 13 and 26 pS subconductance states gated independently. The disulfide cross-linking agent DTNB restored the wild-type gating pattern to R567*X* αbENaC. *Each panel* is representative of at least five separate experiments, the holding potential was +100 mV, and *dashed lines* represent the zero current level.

These observations led us to propose a model whereby both the αrENaC and αβγrENaC Na^+ channels behaved functionally as a triple-barreled ion channel. In the case of αrENaC, the channel was proposed to comprise three 13 pS conductive pores that, when gating cooperatively, gave rise to a 39 pS conductance level. Based on our experimental observations with high salt and DTT, we suggested a simple model whereby two of these barrels would be linked by disulfide bonds and the third barrel might interact with the covalently linked pair by electrostatic mechanisms that would be subject to disruption by high salt.

However, when we incorporated the highly homologous bovine isoform of αrENaC, αbENaC, into planar lipid bilayers, we observed a different gating pattern, namely a single step transition of 39 pS interspersed by long closed periods. Comparison of the amino acid sequences of αrENaC with αbENaC showed that there was a significant region of diversity at the extreme C terminus. The present series of experiments were therefore undertaken to determine whether the site of the kinetic differences in gating pattern between αrENaC and αbENaC resided in the C-terminal region. We found that premature truncation of αbENaC just after the end of the second hydrophobic domain and 17 amino acid residues prior to the initiation of the greatest sequence divergence effectively converted the gating pattern of αbENaC to one that was indistinguishable from that which we had previously reported for αrENaC. In contrast, the equivalent C-terminal truncation, when executed in αrENaC, had no effect on the pattern of αrENaC channel gating. However, in other respects (such as the response to DTT, high salt, cross-linking with DTNB, amiloride sensitivity, and ion selectivity), wild-type, R567*X* αbENaC, and R613*X* αrENaC behaved identically to wild-type αrENaC.

These results suggest that a triple-barreled model could also account for the behavior of wild-type αbENaC and that the region responsible for the different gating behavior of αbENaC resides within the extreme C terminus; however, the minimum region required to maintain the gating characteristics of αbENaC remains to be determined. In contrast, the C-terminal region of αrENaC seems to exert no influence on the gating behavior of this prototypical ENaC isoform. We would also predict that the human homolog, αhENaC, which shares a much greater C-terminal homology with αrENaC than does αbENaC (3, 13), would also not be subject to C-terminal-based modification of its gating pattern. In contrast, an alternatively spliced form of αrENaC that has been detected in taste tissues, kidney, and lung has a significant (199 amino acid) deletion at the C terminus (18). This splice variant, which is missing the second transmembrane domain of the channel, was associated with no significant increase in amiloride-sensitive Na^+ current when heterologously expressed in *Xenopus* oocytes (18).

Our results with the cross-linking agent DTNB, together with our results using DTT, suggest that the residues important for cross-linking lie predominantly in the N terminus because DTNB and DTT were as effective in either restoring or disrupting triple-barreled behavior of the channel in the truncation mutants as they were in the wild-type αENaC channels. However, the C terminus of αbENaC does contain a number of charged residues that are not present in αrENaC, which may influence the gating behavior of the channel. Given the reducing environment of the cytosol, the way in which the N terminus of the αENaC subunit may cross-link to other subunits or even other associated proteins is at present unknown, as is the

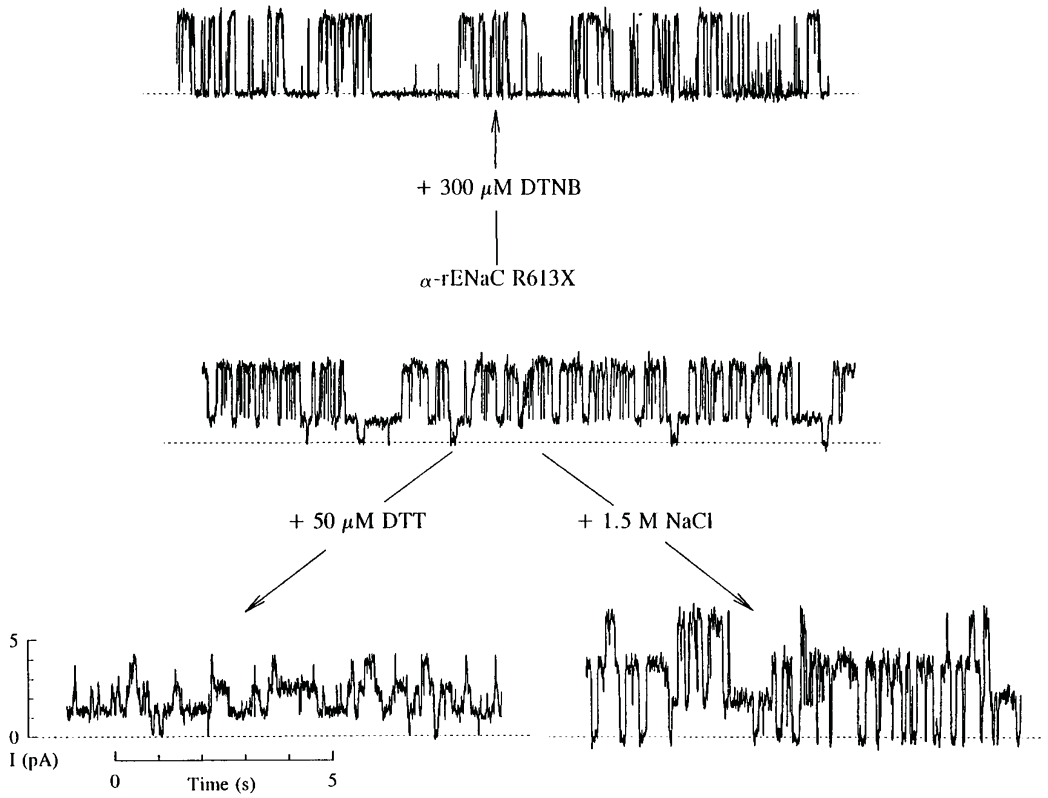

FIG. 6. **Effect of sulfhydryl-active agents and high salt on R613*X* αrENaC.** The addition of DTT to R613*X* αrENaC also caused the gating behavior of this truncated protein to resolve into three independently gated 13 pS subconductance levels. The presence of 1.5 M NaCl similarly caused the 13 and 26 pS transition steps to gate independently such that we could observe the 26 pS state in the absence of an initial transition to 13 pS. Cross-linking R613*X* αrENaC with DTNB also changed the gating behavior of the truncated protein, causing a predominance of single-step 39 pS transitions. *Panels* are representative of six separate experiments, the holding potential was +100 mV, and *dashed lines* represent the zero current level.

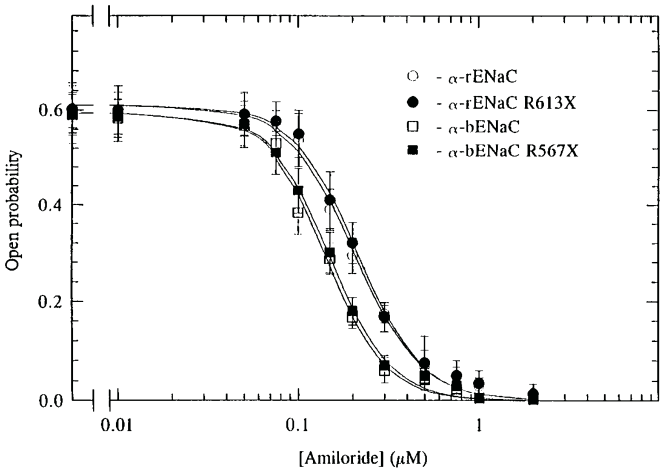

FIG. 7. **Dose-response curve of amiloride on wild-type and truncated αbENaC and αrENaC.** The K^+-sparing diuretic amiloride caused a dose-dependent reduction in channel open probability in both αbENaC and αrENaC. Although the curve for the effect of amiloride on αbENaC was shifted slightly to the left of that for αrENaC, this shift was not significant. The amiloride sensitivity of each isoform was not affected by C-terminal truncation. Results are the means of four separate determinations and are expressed ± S.D.

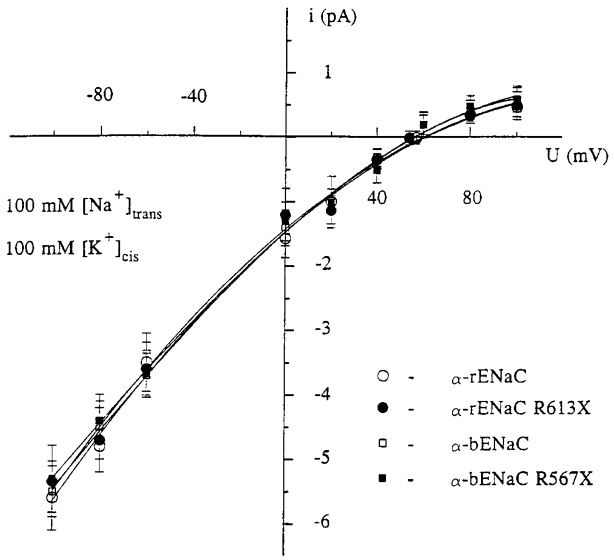

FIG. 8. **Ion selectivity of wild-type and truncated bovine and rat ENaC isoforms.** The ion selectivity of wild-type and mutant ENaC isoforms was determined under biionic conditions with 100 mM Na^+ in the *trans* compartment and 100 mM K^+ in the *cis* chamber. Under these conditions, we calculated a P_{Na}:P_K ratio of approximately 10:1 using the Goldman-Hodgkin-Katz constant field equation. Both isoforms and their respective truncations yielded an identical permeability ratio. Values are the mean of at least four separate determinations ± S.D.

exact subunit stoichiometry of the assembly of the channel. However, our earlier studies do suggest that multiple αENaC subunits may contribute to the overall conformation of the αβγENaC channel complex (9).

In summary, therefore, we have demonstrated that the unique kinetic signature of αbENaC is conferred by the highly divergent C terminus of this protein. Truncation of this region in αrENaC has no effect on gating of this rat αENaC isoform, and in either isoform, no property so far examined is affected by deletion of the C terminus other than the gating pattern of αbENaC.

Acknowledgments—We thank Christie Brown for excellent assistance with the expression of ENaC cRNAs in *Xenopus* oocytes and Elizabeth Fernandez for superb technical assistance.

REFERENCES

1. Canessa, C. M., Horisberger, J.-D., and Rossier, B. C. (1993) *Nature* **361,** 467–470
2. Canessa, C. M., Schild, L., Buell, G., Thorens, B., Gautschi, I., Horisberger, J.-D., and Rossier, B. C. (1994) *Nature* **367,** 463–467
3. McDonald, F. J., Snyder, P. M., McCray, P. B., Jr., and Welsh, M. J. (1994) *Am. J. Physiol.* **266,** L728–L734
4. McDonald, F. J., Price, M. P., Snyder, P. M., and Welsh, M. J. (1995) *Am. J. Physiol.* **268,** C1157–C1163
5. Lingueglia, E., Voilley, N., Waldman, R., Lazdunski, M., and Barbry, P. (1993) *FEBS Lett.* **318,** 95–99
6. Bradford, A. L., Ismailov, I. I., Achard, J.-M., Warnock, D. G., Bubien, J. K., and Benos, D. J. (1995) *Am. J. Physiol.* **269,** C601–C611
7. Puoti, A., May, A., Canessa, C. M., Horisberger, J.-D., Schild, L., and Rossier, B. C. (1995) *Am. J. Physiol.* **269,** C188–C197
8. Voilley, N., Lingueglia, E., Champigny, G., Mattei, M. G., Waldmann, R., Lazdunski, M., and Barbry, P. (1994) *Proc. Natl. Acad. Sci. U. S. A.* **91,** 247–251
9. Ismailov, I. I., Awayda, M. S., Berdiev, B. K., Bubien, J. K., Lucas, J. E., Fuller, C. M., and Benos, D. J. (1996) *J. Biol. Chem.* **271,** 807–816
10. Price, M. P., Snyder, P. M., and Welsh, M. J. (1996) *J. Biol. Chem.* **271,** 7879–7882
11. Waldmann, R., Champigny, G., Bassilana, F., Voilley, N., and Lazdunski, M. (1995) *J. Biol. Chem.* **270,** 27411–27414
12. Lingueglia, E., Champigny, G., Lazdunski, M., and Barbry, P. (1995) *Nature* **378,** 730–733
13. Fuller, C. M., Awayda, M. S., Arrate, M. P., Bradford, A. L., Morris, R. G., Canessa, C. M., Rossier, B. C., and Benos, D. J. (1995) *Am. J. Physiol.* **269,** C641–C654
14. Laemmli, U. K. (1970) *Nature* **227,** 680–685
15. Awayda, M. S., Ismailov, I. I., Berdiev, B. K., and Benos, D. J. (1995) *Am. J. Physiol.* **268,** C1450–C1459
16. Perez, G., Lagrutta, A., Adelman, J. P., and Toro, L. (1994) *Biophys. J.* **66,** 1022–1027
17. Cunningham, S. A., Awayda, M. S., Bubien, J. K., Ismailov, I. I., Arrate, M. P., Berdiev, B. K., Benos, D. J., and Fuller, C. M. (1995) *J. Biol. Chem.* **270,** 31016–31026
18. Li, X.-J., Xu, R.-H., Guggino, W. B., and Snyder, S. H. (1995) *Mol. Pharmacol.* **47,** 1133–1140